Final

Project Technical Report

of ISTC 2102p

Development of Liquid Crystal Spatial Light Modulators for mid-IR Radiation, Addressed by Visible Radiation

(from 1 September 2001 to 31 August 2002 for 12 months)

Vladimir Yurievitch Venediktov
(Project Manager)

Federal State Unitary Enterprise
Scientific Research Institute for Laser Physics

October 2002

The work was financially supported by Partner Project with EOARD, USA, and contract with International Science and Technology Center (ISTC), Moscow

REPORT DOCUMENTATION PAGE

Form Approved OMB No. 0704-0188

1. REPORT DATE *(DD-MM-YYYY)*	2. REPORT TYPE	3. DATES COVERED *(From – To)*
07-01-2003	Final Report	17-Sep-01 - 14-Jan-03

4. TITLE AND SUBTITLE

Development of Liquid Crystal Spatial Light Modulators for mid-IR Radiation, Addressed by Visible Radiation

5a. CONTRACT NUMBER
ISTC Registration No: 2102p

5b. GRANT NUMBER

5c. PROGRAM ELEMENT NUMBER

6. AUTHOR(S)

Mr. Vladimir Venediktov

5d. PROJECT NUMBER

5d. TASK NUMBER

5e. WORK UNIT NUMBER

7. PERFORMING ORGANIZATION NAME(S) AND ADDRESS(ES)

Research Institute for Laser Physics
Birjevaya 12
St. Petersburg 199034
Russia

8. PERFORMING ORGANIZATION REPORT NUMBER

N/A

9. SPONSORING/MONITORING AGENCY NAME(S) AND ADDRESS(ES)

EOARD
PSC 802 BOX 14
FPO 09499-0014

10. SPONSOR/MONITOR'S ACRONYM(S)

11. SPONSOR/MONITOR'S REPORT NUMBER(S)
ISTC 00-7024

12. DISTRIBUTION/AVAILABILITY STATEMENT

Approved for public release; distribution is unlimited.

13. SUPPLEMENTARY NOTES

14. ABSTRACT

This report results from a contract tasking Research Institute for Laser Physics as follows: Recent years has shown fast progress in the development of the technique of compensation for distortions in laser and imaging optical systems working in the visible spectral range through the use of dynamic holographic recording in optically-addressed liquid crystal spatial light modulators. However, this has not been extended to the mid-IR due to the lack of photoconductors that are sensitive to radiation in this wavelength range. The goal of this project is to solve this problem with an approach that will result in the photoconductive layer being transparent to the mid-IR raidation, and with the internal mirror that reflects the mid-IR radiation being sufficiently transparent to the visible light that the hologram can be recorded. Several elements of this type will be fabricated, tested and delivered. The spatial light modulator is to provide high diffraction efficiency for the recording of the dynamic grating, and to possibly record the phase gratings with the amplitude of the phase retardation of as much as 2 pi radians in the mid-IR spectral range.

15. SUBJECT TERMS
EOARD, Physics, Optics

16. SECURITY CLASSIFICATION OF:			17. LIMITATION OF ABSTRACT	18, NUMBER OF PAGES	19a. NAME OF RESPONSIBLE PERSON
a. REPORT	b. ABSTRACT	c. THIS PAGE			Alexander J. Glass, Ph. D.
UNCLAS	UNCLAS	UNCLAS	UL	36	19b. TELEPHONE NUMBER *(Include area code)* +44 (0)20 7514 4953

Table of content

Introduction

The goal of work was to develop and to fabricate liquid crystal spatial light modulators (LC SLMs) with the mirror geometry, addressed by visible radiation and controlling mid-IR radiation (3-4 microns). The elements were to provide high diffraction efficiency for the recording of dynamic gratings and the possibility to record phase gratings with an amplitude of phase retardation of up to 2π in the specified spectral range.

The expected parameters of SLMs to be fabricated were as follows

clear aperture	20 mm
optical quality	at least quarter wave
geometry of SLM	with mirror
wavelength of record	0.45-0.70 micron
reading out wavelength	3-4 microns
spatial resolution	10-20 lp/mm
diffraction efficiency	10 - 15%
phase retardation in spectral range 3-4 μm	up to 2π

In course of work were carried out the following tasks:

- were optimized the parameters of the mirror, photoconductor and nematic LC so as to provide high diffraction efficiency;
- were minimized light loses on the boundaries of the media that comprise the SLM;
- the parameters of SLMs were tested and three specimens were delivered to the Customer.

The work consisted of four stages:

1. Analysis of existing technology of OA LC SLMs for IR radiation and of their possible application for holographic correction.
2. Elaboration of novel technology of OA LC SLMs for mid-IR radiation, addressed by visible light.
3. Development and creation of laser setup, emitting in mid-IR for testing of created OA LC SLM elements.
4. Fabrication and testing of OA LC SLMs for mid-IR radiation, addressed by visible light.

1. Analysis of existing technology of OA LC SLMs for IR radiation and of their possible application for holographic correction.

Recent years have brought a significant progress in application of dynamic holography for the real-time correction of distortions in various kinds of optical systems. Especially spectacular results (see, for example, [1-3]) were demonstrated with the use of thin dynamic holograms in the optically addressed liquid crystal spatial light modulators (OA LC SLMs, see Fig.1) [4-6]. These sandwich-like devices comprise several layers, main of which are the layers of photoconductor and of the liquid crystal (LC). When the photoconductor layer is illuminated by the pattern of interference of the reference wave and the signal wave, bearing the information about the distortions of the optical system to be corrected, the conductivity of photoconductor in the illuminated zones changes, leading to the redistribution of feeding voltage and thus to the modulation of optical properties of LC (of its birefringence). As a result in LC layer is recorded the efficient thin dynamic hologram. Reconstruction of this hologram by the light wave, distorted by the same optical system, results in subtraction of distortions impact to the phase modulation of this wave, providing thus an opportunity to form a high quality corrected image. In the said papers and in some other experiments this approach was successfully applied to distortions correction in the visible range of spectrum.

Unfortunately, in the practically important IR-range of spectrum the application of this method in its classical way is impossible due to the absence of LC-modulators, addressed by IR-radiation. Historically all such elements were designed only on the basis of photoconductors, sensitive only to the visible light. One can treat creation of the modulators, sensitive to near-IR radiation (1-1.5 μm) as the prospective technological task (not solved yet), however, the realization of the elements for the mid-IR range (1.5-10 μm) applications seems hardly possible in the nearest future. At the same time it is quite possible to create the LC-modulators, read-out by radiation of the said spectral ranges.

We have proposed [7] to solve this problem in the more sophisticated scheme of corrector record, based on the so-called two-wavelength holography principle. In this scheme it is possible to record the dynamic holographic corrector of distortions, working in mid-IR range of spectrum, with the use of visible radiation. There also exists one more approach to the record of such corrector, whose scheme is very

similar to that of experiments [8,9]. In the said papers the interference pattern of signal and reference waves was registered by the matrix photo sensor, reconstructed at the projection display and then, with the use of auxiliary light source, was transferred to the photosensitive layer of dynamic holographic corrector, based on OA LC SLM. In the papers [8,9] the projection display has reconstructed the interference pattern, subjected to a special digital processing (asymmetrization), providing thus an opportunity to increase the diffraction efficiency of hologram-corrector. However, the same scheme (with asymmetrization or without) can be used also for the corrector record in IR range of spectrum. For this spectral range exist rather efficient and high-resolving matrix photo sensors, and the image transfer from the projection display to the hologram can be realized with the use of visible light.

Hence, creation of the LC SLMs for the record of dynamic holograms by visible radiation, but with the possibility of their reading-out by IR-radiation, is a prospective and actual task. Earlier, within the scope of our studies on two-wavelength dynamic holography [7] we have created and tested first specimens of such modulators. They comprised the standard scheme (see Fig.1.1) and were working in transmission mode (i.e. lacking the internal mirror and the light-absorption layer). The glass is not transparent in mid-IR range of spectrum, and thus the substrata were made of BaF_2 crystal. The phase modulation of light was provided by S-effect in nematic LC. Chalkogenide glass was used as the photoconductor. The dynamic holograms in such modulators were recorded by visible radiation of Ar-ion laser and read out by radiation of CW CO_2-laser (λ=10 μm). In these devices the diffraction efficiency to the first order of diffraction was equal some 1-2%.

The goal of this work is the creation on the base of previous experience of similar OA LC SLMs for dynamic holography in the practically important spectral range 2.5-5 μm with the sufficiently high diffraction efficiency (10-20%) and also with the possibility of deep (up to 2π) phase modulation, providing the application in the said spectral range of “blazed” dynamic holography technique [8,9] and thus of further increase of the diffraction efficiency due to assymetrization of the holographic fringe profile. The architecture of such elements is considered in Section 2.

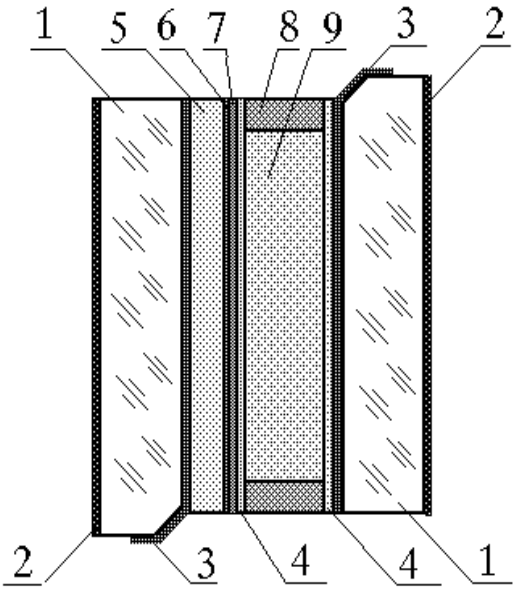

Fig.1.1. Standard design of OA LC SLM: 1 – plain glass substrata, 2 – AR coating, 3 – transparent electrodes, fed by voltage, 4 – orientation coating, 5 – photoconductor, 6 – light absorption layer, 7 – internal mirror, 8 – spacers, 9 – liquid crystal.

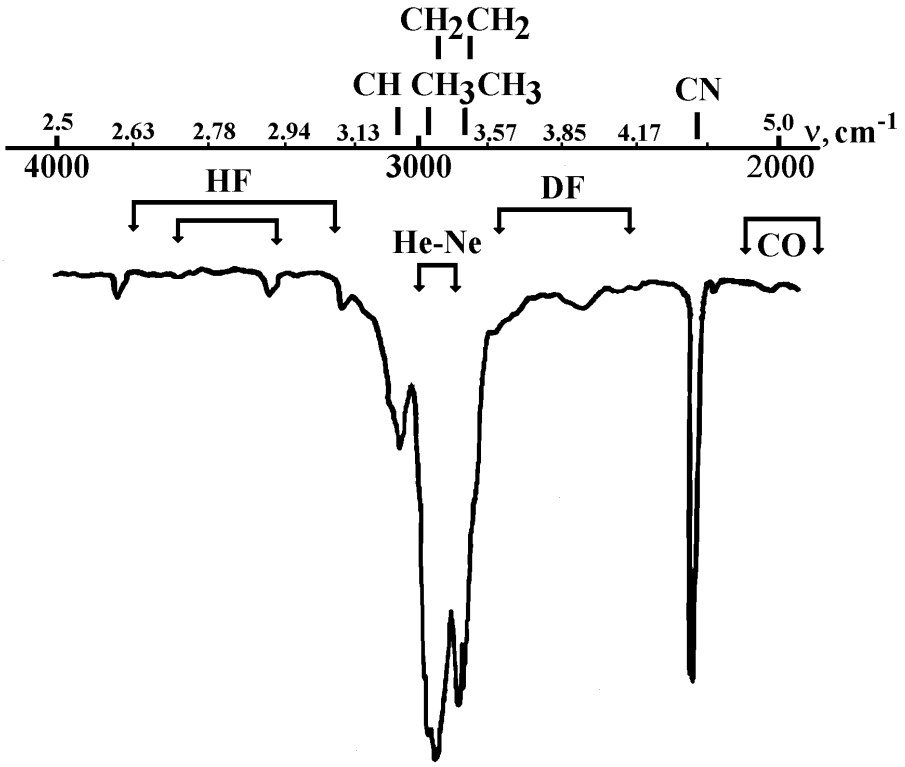

Fig.1.2. Spectrum of LC composition transmission. Wavelengths are given in μm (upper scale) and in inverted centimeters (lower scale). In the upper part of the Figure are indicated the organic chemical radicals, responsible for the absorption lines, the arrows indicate the wavelengths or spectral ranges of generation of the most important lasers, emitting in the spectral range under consideration.

In the Fig.1.2 is shown the typical spectrum of LC composition transmission in the spectral range under consideration. One can see that it is mostly transparent with the exception of the range from 3 to 3.5 μm. The latter range is also interesting, but the strong absorption by hydrocarbons in this range prevents application of OA LC SLMs in corresponding laser systems. At the same time it is well known that the isotope replacement leads to shift of frequencies of oscillations of atoms and of molecular fragments. The most prospective for solution of these tasks is deuterization of molecules, becose replacement of hydrogen atoms by deuterium leads to relatively strong variation of atomic mass and thus to strong shift of molecular oscillation frequencies. To reveal the possibility to use the deuterized LC in future OA LC SLMs, applicable in the said spectral range, in course of current study was carried out the calculation of oscillatory frequencies and determining of the absorption spectra for the typical LC molecules, in which hydrogen atoms are replaced by deuterium.

General majority of liquid crystals are the multicomponent mixtures. The LC compositions have rather complicated content, but all molecules of such compositions are combined by combinations of limited number of functional groups. In the spectral range of mid-IR (3-5 μm) are positioned the bands of valence oscillations of CH, CH_2 and CH_3 groups, i.e. practically all organic compounds are non-transparent in this spectral range. Investigation of characteristical bands of absorption for various types of hydrocarbon structures has established the reliable relationship between the types of corresponding groups and of band position. These absorption bands are placed as a compact group nearby the frequency band around 3000 cm^{-1}.

Group CH_3. In all cases provides two intense bands at 2962 and 2872 cm^{-1}, corresponding to the symmetrical and asymmetrical valence oscillations.

Group CH_2. This group provides two characteristical bands at 2926 and 2853 cm^{-1}, corresponding to the symmetrical and asymmetrical valence oscillations.

Group CH. Intensity of absorption by this group at 2890 cm^{-1} is much less than that of the bands, mentioned above.

Valence oscillations of **CH in aromatic compounds** correspond to the bands (usually three) nearby 3038 cm^{-1}. The intensity of these bands is significantly lower than that of oscillations of CH_2 in extreme compounds.

Modification of the aggregate state results in some shift of the bands with respect to above given values. In the Fig.1.3 is shown the structural formula of pentilcyanbifenil, which is the basis of numerous LC compositions.

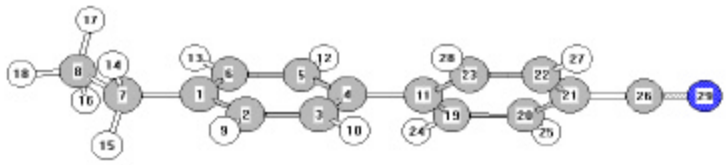

Fig.1.3. Structural formula of pentilcyanbifenil

However, one can obtain the calculated spectra, which are adequate to the real spectral features, by means of theoretical investigation of much simpler molecule of ethylbenzene, shown in the Fig.1.4.

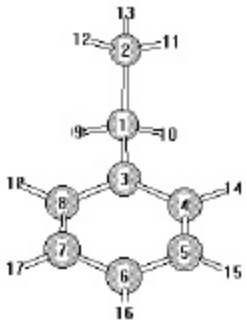

Fig.1.4. Molecule of ethylbenzene

This molecule contains all types of hydrocarbon groups, presented in all molecular structures. Further complication of structure does not lead to some significant modification of lengths of bends and of molecular force constants. So the results, obtained for this molecule, can be extrapolated onto more complicated compounds. In the case of nitril compounds one has to expect also observation of IR absorption bands in the range of tripled bends oscillations 2200 – 2300 cm^{-1}. Analysis of influence of **CN** group would result only in increase of calculation time, but would not influence onto calculation results.

Calculation of molecular spectra was carried out with the use of code Gaussian 98 [10] with the use of method of density functional theory (DFT) B3PW91 with the gradient correction [11] for the exchange interaction and with the correction, taking into account the electron correlation. [12]. For all atoms was chosen the standard basis set 6-311G** with the split valence and with polarization functions. Geometry parameters were optimized within the molecular symmetry model C1. Calculation of oscillation frequencies did not reveal the imaginary values for frequencies. The force field, which was determined, was used for calculation of diagonal elements of potential energy distribution matrix, providing evaluation of all oscillatory frequencies of molecules under study.

RESULTS OF THE NORMAL COORDINATE ANALYSIS

***Cartesian coordinates in original axes**:*

Atom	**Mass**	X	Y	Z
1 C1	12.000000	1.970972	-.073605	.378545
2 C2	12.000000	2.232831	1.006959	1.433211
3 C3	12.000000	.520238	-.155597	-.025482
4 C4	12.000000	-.370620	-.981907	.663699
5 C5	12.000000	-1.716446	-1.032732	.316159
6 C6	12.000000	-2.197163	-.254264	-.731812
7 C7	12.000000	-1.321316	.572310	-1.428242
8 C8	12.000000	.023533	.619096	-1.076458
9 H9	2.014100	2.583404	.127194	-.507137
10 H10	2.014100	2.295313	-1.045471	.765940
11 H11	2.014100	1.653774	.816165	2.341210
12 H12	2.014100	1.946545	1.994686	1.060997
13 H13	2.014100	3.291579	1.041199	1.706823
14 H14	2.014100	-.002846	-1.597760	1.480009
15 H15	2.014100	-2.390378	-1.685402	.862049
16 H16	2.014100	-3.245978	-.294837	-1.006747
17 H17	2.014100	-1.685195	1.179242	-2.251276
18 H18	2.014100	.701612	1.263425	-1.629591

Principal moments:

Ix= 139.320993 Iy= 410.737813 Iz= 496.167368

Cartesian coordinates in principal axes:

Atom	Mass	X	Y	Z
1 C1	12.000000	1.918977	-.000507	-.590154
2 C2	12.000000	2.750098	.000369	.697381
3 C3	12.000000	.434041	-.000227	-.326422
4 C4	12.000000	-.268827	1.198514	-.183657
5 C5	12.000000	-1.631541	1.201715	.094940
6 C6	12.000000	-2.318458	.000255	.236301
7 C7	12.000000	-1.631900	-1.201454	.095298
8 C8	12.000000	-.269225	-1.198716	-.183391
9 H9	2.014100	2.180563	-.878336	-1.190831
10 H10	2.014100	2.180840	.876332	-1.192131
11 H11	2.014100	2.529041	.882224	1.305359
12 H12	2.014100	2.531417	-.882306	1.304975
13 H13	2.014100	3.821156	.001835	.474186
14 H14	2.014100	.258438	2.141808	-.298043
15 H15	2.014100	-2.159121	2.144775	.197199
16 H16	2.014100	-3.382144	.000422	.450357
17 H17	2.014100	-2.159778	-2.144312	.197876
18 H18	2.014100	.257883	-2.142145	-.297435

62 internal coordinates:

18 bond stretches, bond length in A

1. C1 C2 1.53249
2. C1 C3 1.50817
3. C1 H9 1.09537
4. C1 H10 1.09535
5. C2 H11 1.09370
6. C2 H12 1.09367
7. C2 H13 1.09407
8. C3 C4 1.39692
9. C3 C8 1.39693
10. C4 C5 1.39090

11. C4 H14 1.08669
12. C8 C7 H17 1.39117
13. C5 H15 1.08543
14. C6 C7 1.39117
15. C6 H16 1.08501
16. C7 C8 1.39088
17. C7 H17 1.08543
18. C8 H18 1.08670

30 angle bends, angle in deg

19. C2 C1 C3 112.772
20. C2 C1 H9 109.370
21. C2 C1 H10 109.367
22. C3 C1 H9 109.340
23. C3 C1 H10 109.350
24. H9 C1 H10 106.443
25. C1 C2 H11 110.970
26. C1 C2 H12 110.968
27. C1 C2 H13 111.072
28. H11 C2 H12 107.548
29. H11 C2 H13 108.071
30. H12 C2 H13 108.069
31. C1 C3 C4 120.893
32. C1 C3 C8 120.892
33. C4 C3 C8 118.194
34. C3 C4 C5 121.024
35. C3 C4 H14 119.341
36. C5 C4 H14 119.634
37. C4 C5 C6 120.141
38. C4 C5 H15 119.807
39. C6 C5 H15 120.052
40. C5 C6 C7 119.475
41. C5 C6 H16 120.264
42. C7 C6 H16 120.261
43. C6 C7 C8 120.140
44. C6 C7 H17 120.050
45. C8 C7 H17 119.809
46. C3 C8 C7 121.026
47. C3 C8 H18 119.334

48. C7 C8 H18 119.639

6 out of plane bends, non-planarity in deg

49. C3 C1 C4 C8 Central atom: C3 o.o.p. 1.418
50. C4 C3 C5 H14 Central atom: C4 o.o.p. .298
51. C5 C4 C6 H15 Central atom: C5 o.o.p. .252
52. C6 C5 C7 H16 Central atom: C6 o.o.p. .241
53. C7 C6 C8 H17 Central atom: C7 o.o.p. .253
54. C8 C3 C7 H18 Central atom: C8 o.o.p. -.286

8 torsions, angle in deg

55. C3 C1 C2 H11 -59.662
56. C2 C1 C3 C4 89.116
57. C1 C3 C4 C5 -178.271
58. C1 C3 C8 C7 178.266
59. C3 C4 C5 C6 .000
60. C4 C5 C6 C7 -.073
61. C5 C6 C7 C8 .068

POTENTIAL ENERGY DISTRIBUTION, %

Further tables contain the frequencies of the most intense oscillations and the impact to the potential energy of atoms, correspondingly numbered in the molecule scheme.

14 **856.633**

21 (50) . C4 C3 C5 H14 Central atom: C4
21 (54) C8 C3 C7 H18 Central atom: C8
18 (51) C5 C4 C6 H15 Central atom: C5
18 (53) C7 C6 C8 H17 Central atom: C7

15 **922.142**

25 (50) C7 C6 C8 H17 Central atom: C7
25 (54) C8 C3 C7 H18 Central atom: C8
22 (52) C6 C5 C7 H16 Central atom: C6

17 981.705

64 (1) C1 C2

18 1000.955

25 (52) C6 C5 C7 H16 Central atom: C6
20 (51) C5 C4 C6 H15 Central atom: C5
20 (53) C7 C6 C8 H17 Central atom: C7

20 1055.014

26 (12) C5 C6

25 (14) C6 C7

21 1056.380

18 (22) C3 C1 H9
18 (23) C3 C1 H10

22 1083.442

33 (1) C1 C2
27 (27) . C1 C2 H13

23 1119.101

11 (16) C7 C8
11 (10) C4 C5

28 1351.733

19 (21) C2 C1 H10
19 (20) . C2 C1 H9

31 1404.355

16 (30) H12 C2 H13
16 (29) H11 C2 H13
15 (25) C1 C2 H11
15 (26) C1 C2 H12

32 1484.021

52 (24) H9 C1 H10
22 (28) H11 C2 H12

33 1484.995

12 (42) C7 C6 H16
12 (41) C5 C6 H16
12 (16) C7 C8
12 (10) C4 C5

34 1491.095

45 (29) H11 C2 H13
45 (30) H12 C2 H13

35 1501.873

37 (28) H11 C2 H12
29 (24) H9 C1 H10

36 1529.460

8 (14) C6 C
8 (38) C4 C5 H15
8 (45) C8 C7 H17
8 (12) C8 C7 H17

37 1638.855

19 (12) C8 C7 H17
19 (14) C6 C
15 (8) C3 C4
15 (9) C3 C8

38 1660.785

20 (16) C7 C8
20 (10) C4 C5

39 3034.957

35 (7) . C2 H13
31 (5) . C2 H11
31 (6) C2 H12

40 3038.805

48 (3) C1 H9
48 (4) C1 H10

41 3075.572

44 (4) C1 H10
44 (3) C1 H9

42 3110.083

62 (7) . C2 H13
19 (5) C2 H11
17 (6) C2 H12

43 3115.236

45 (6) C2 H12
43 (5) C2 H11

44 3162.529

32 (18) C8 H18
32 (11) C4 H14

45 3163.859

42 (11) C4 H14
42 (18) C8 H18

46 3177.643

43 (15) C6 H16

47 3186.554

42 (13) C5 H15
42 (17) C8 H18

48 3199.517

49 (15) C6 H16
22 (17) C8 H18
22 (13) C5 H15

Hence, one can see that the maximal impact to the spectral range under study is provided by symmetrical and asymmetrical oscillations of **CH** groups of benzene ring and of alkyl radical. In the Fig.1.5 and Fig.1.6 are shown the calculated spectra for usual ethylbenzene and the one, where hydrogen is replaced by deuterium.

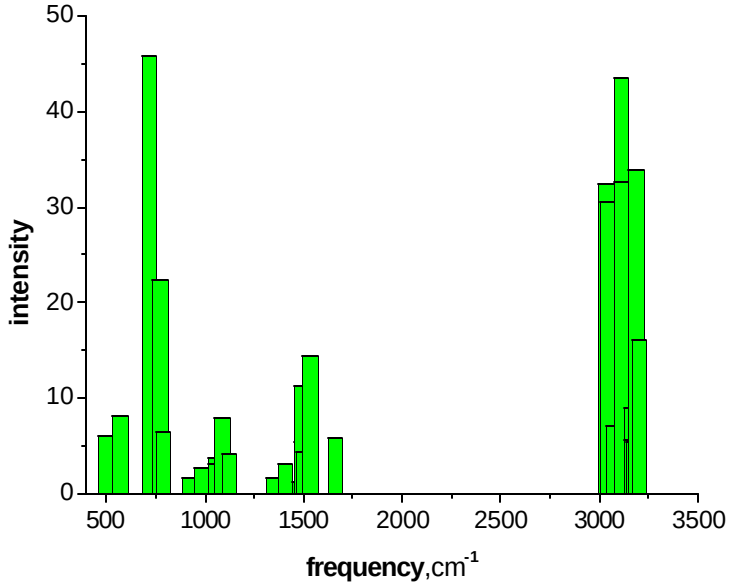

Fig.1.5. Spectrum of oscillation frequencies for the ethylbenzene with hydrogen

Oscillation frequencies for compound with hydrogen

1 50.096	**2** 136.929	**3** 219.012
4 309.002	**5** 354.853	**6** 412.950
7 499.530	**8** 565.728	**9** 632.469
10 715.583	**11** 768.080	**12** 786.636

13	789.809	**14**	856.633	**15**	922.142
16	979.754	**17**	981.705	**18**	1000.955
19	1016.808	**20**	1055.014	**21**	1056.380
22	1083.442	**23**	1119.101	**24**	1178.391
25	1199.840	26	1231.634	27	1269.700
28	1351.733	29	1353.027	30	1362.692
31	1404.355	32	1484.021	33	1484.995
34	1491.095	35	1501.873	36	1529.460
37	1638.855	38	1660.785	**39**	**3034.957**
40	**3038.805**	**41**	**3075.572**	**42**	**3110.083**
43	**3115.236**	**44**	**3162.529**	**45**	**3163.859**
46	**3177.643**	**47**	**3186.554**	**48**	**3199.517**

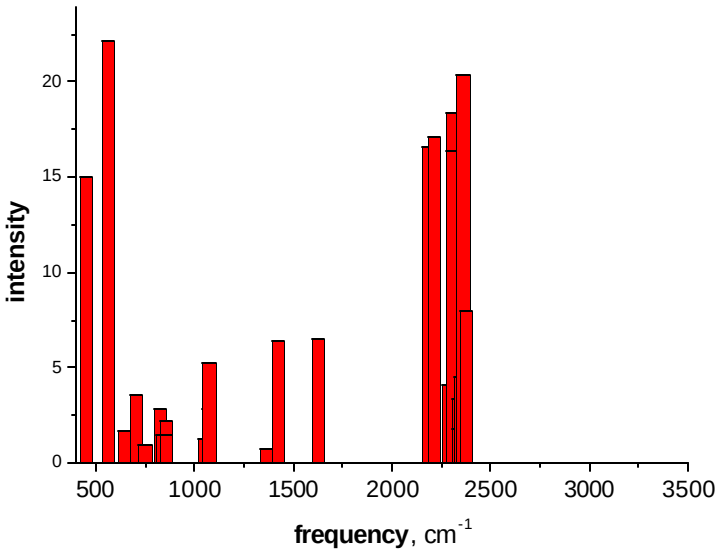

Fig.1.6. Spectrum of oscillation frequencies for the ethylbenzene with hydrogen, replaced by deuterium

Oscillation frequencies for compound with deuterium

1	42.566	**2**	122.814	**3**	159.450
4	275.804	**5**	296.035	**6**	359.023
7	446.005	**8**	500.238	**9**	559.082
10	588.416	11	606.280	12	644.189
13	666.665	14	701.660	15	749.592
16	797.071	17	805.351	18	827.156
19	835.502	20	839.564	21	853.879
22	854.111	23	880.423	24	923.236
25	974.467	26	983.808	27	1044.652
28	1057.828	29	1073.127	30	1073.212

31	1087.598	32	1144.465	33	1224.460
34	1345.379	35	1363.733	36	1421.842
37	1601.834	38	1628.**744**	**39**	**2180.454**
40	**2211.901**	**41**	**2281.479**	**42**	**2304.076**
43	**2307.747**	**44**	**2331.598**	**45**	**2335.056**
46	**2348.405**	**47**	**2359.342**	**48**	**2373.254**

Hence, the calculations, which were carried out that the absorption spectra of structures, where hydrogen is replaced by deuterium, do not contain the bands with the wavelengths of shorter than 2400 cm^{-1} or 4.16 μm, promising in future the possibility of synthesis of desired deuterated LC and creation of OA LC SLMs for spectral range 3-3.5 μm.

2. Elaboration of novel technology of OA LC SLMs for mid-IR radiation, addressed by visible light.

Asymmetrization of the fringe profile is possible only in modulators with the so-called "gray" scale dependence of phase modulation upon intensity of recording radiation. Thus we are to use in the developed modulators the S-effect in nematic LC. In nematics of various composition the magnitude of refraction index modulation due to birefringence is equal $\Delta n=0.12 - 0.25$. Hence, provision of phase modulation depth $\Delta\Phi=2\pi$ at the wavelength 5 μm the thickness of LC layer has to be some 20-40 μm. We use in the developed elements the nematics with the maximal available value of Δn, however, even the layer thickness of ~ 20 μm is very high. One can reduce in twice in the modulator with the internal mirror.

Now there exist two approaches to the design of internal mirrors in OA LC SLMs. The traditional approach is based on the use of mosaic of metallic mirrors. However, upon the base of previous experience, it is not applicable in OA LC SLMs for the record of dynamic holograms due to the too strong light scattering. Recently for the OA LC SLMs, working in the visible spectral range, were developed the multi-layer dielectric coatings (see, for example, [5,6]). However, in the case of mid-IR range of spectrum, the thickness of such mirrors seems to be also too high. To solve this problem within the scope of this work we have proposed to implement for the first time a new architecture of SLM. It is well known, that the thin (thickness < 1 μm) layers of some metals, gold, for instance, are practically transparent for the visible light, but have a rather high reflectivity in the mid-IR range. We have deposited onto BaF_2 and tested the layers of gold with the thickness ~ 0.1 μm. In the visible light their transparency was as high as 50-70%, while in the spectral range 2-5 μm their reflectivity was as high as 70-80%. Thus we have proposed to depose in the designed modulators the mirror layer not between the layers of photoconductor and LC (as in the Fig.1.1), but between the substratum and the photoconductor layer. The light-absorbing layer in this case is not used. The dynamic hologram is recorded by visible light through the gold layer, while its' reading out by IR radiation is done in a mirror geometry. The said layer of gold can bear also an auxiliary function of conductive layer (instead of transparent electrode) for the delivery of feeding voltage.

Application of the thick (10 and more micron) LC layers limits the possibility of use of various photoconductors, because the majority of these media, including the now most widely used in OA LC SLMs amorphous silicon and silicon carbide, have insufficiently high dark resistivity. The thick layer of LC has high resistance, which becomes comparable with the dark resistance of photoconductor and this frustrates the electrical conjugation of the layers. That is why we have decide to use in the developed elements the photoconductor on the base of chalkogenide glass with the approximate percentage content As:Se=1:9. The layer thickness is to be optimised in course of the work. At the same time it is well known that the response time of this layer is comparatively large. Thus it is planned to analyse in course of the work the possibility to use in the developed elements the quicker monocrystal layer of BSO ($Bi_{12}SiO_{20}$).

On the base of analysis of the existing technologies of OA LC SLMs was chosen the following architecture of modulators for the record of dynamic holograms by visible radiation and their reading-out by radiation of mid-IR range of spectrum.

The architecture of modulator is shown in the Fig.2.1. The spatial modulators of light on the base of configuration photoconductor – liquid crystal (PC – LC) comprise the multi-layer structure, placed between two substrata: the one from the record side is made of the standard optical glass (K8), while the second one, placed from the reading-out side, is made of barium fluorine (BaF_2). The transparent conducting coatings 4 cover internal sides of both substrata. On the glass substratum is deposited the semi-transparent gold mirror layer 3, and over this layer is deposited the layer of photoconductor 2. Between the layer of photoconductor and the substratum, made of BaF_2, is placed the layer of liquid crystal 1, whose thickness is determined by the spacer 6. On the first stage of work was used the standard and comparatively cheap nematic LC composition #1289, and on the next stages it is planned to use the more expensive crystal with the larger value of Δn. The surfaces, limiting the layer of LC, are covered by the orientation layers 5.

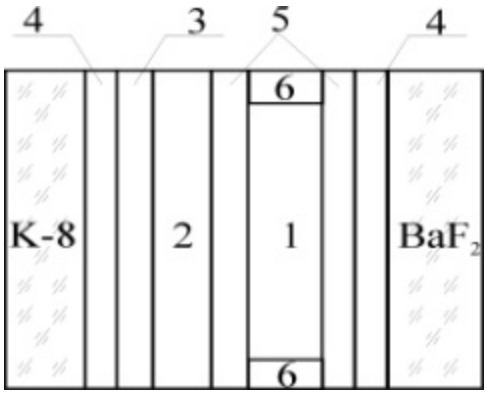

Fig.2.1. Design of OA LC SLM.

Optimization of parameters of layers

1. Transparent conducting layer in the elements under consideration is a standard one and is made of ITO (90 % In_2O_3 + 10 % SnO_2). The layer is deposited by means of cathode deposition in argon atmosphere with the consequent burning out in air. Worth mentioning, that in the device, shown in the Fig.1 one can exclude the layer, deposited onto the glass substratum, because the gold layer is much better conductor. However, it plays the auxiliary helpful role, improving the adhesion of gold to glass and simplifying the mounting of external electric contact.
2. The semi-transparent gold mirror is deposited onto ITO layer on the glass substratum. We have tested the glass films of various thickness. On the first stage it was supposed that the absolute value of glass layer transparency for visible light is not important, because high sensitivity of chalkogenide photoconductor permits to use the layer with transparency $\leq$ 1 %. However, it was determined that the extra thickness of this layer leads to additional problems, because the use of too thick mirror resulted in reduce of diffraction efficiency of modulator. Possible reason is that in the case of too thick mirror (~ 1% transparency), when one has to increase the intensity of recording light in approximately two orders of magnitude (in comparison with the case of mirror absence) the parasitic reflexes from the boundaries glass-air and glass-ITO wash out the recorded holograms. In the case of too thin mirror the large amount of reading-out radiation passes through the modulator, not participating in the reading-out process and heating the glass substratum. In addition, the spectrum of reflection of the reading-out radiation reveals the effects of interference of the mirror, reflected from the mirror and from the photoconductor layer. In other words, the value of mirror reflectivity reveals strong dependence upon the wavelength of radiation and angle of incidence. It was

determined that the optimal thickness of gold layer is the one, whose transparency for green light is ~ 10% and for red light is ~ 5%.

3. The mirror is coated by the layer of photoconductor – of the chalkogenide glass-like semiconductor. For the record at the wavelength λ=0.53 μm the optimal content of this compound is $As_{10}Se_{90}$. Dark resistivity of this compound is very high, and it is not a problem to provide its electrical matching with the thick layer of LC, so in our elements we have used the standard (for usual SLMs, working in the visible light) thickness of PC layer of ~ 1 μm.
4. On the photosensitive layer and on the opposite substratum were placed the orientation layers, made of germanium oxide (GeO), and deposited by method of inclined deposition. The angle of deposition inclination was ~15^o, providing thus the tilt of LC director in ~ 30^o.
5. The substrata were glued in such a manner, that there was preserved the gap to be filled by LC. This gap width is provided by the spacers, made of fluorine polymer. The direction of orientation on both substrata coincides, providing thus the realization of S-effect. LC filling is made in vacuum. The value of LC layer thickness, providing the phase retardation in 2π at 3-4 μm was calculated and tested in experiment. For composition #1289 it is equal ~22-23 μm.

About 20 such elements were fabricated and tested (see Section 4), using two lasers – Er-YAG laser, emitting at 2.94 μm, and the novel type of solid-state laser, emitting at 3.6 μm (see Section 3).

3. Development and creation of laser setup, emitting in mid-IR for testing of created OA LC SLM elements

The task of the reported stage was development of solid-state laser, emitting in spectral range between 3 and 4 μm, for testing modulators.

Yb-Pr:BYF 3.6 mm laser.

For the first time generation at the inter-multiplet transition $^1G_4 \rightarrow {}^3F_4$ of ion Pr^{3+} (λ=3.6 μm) was demonstrated in [13]. There exist the principal difficulties in production of the necessary population of the multiplet $^1G_4$ level by the traditional methods of lamp pumping, and thus for the generation excitation were chosen the ytterbium fluorides $LiYbF_4$ and $BaYb_2F_8$, where the ions of Yb^{3+} are the snsitizing ions (transitions $^3H_4 \rightarrow {}^1G_4$ of Pr^{3+} ion and $^2F_{5/2} \rightarrow {}^2F_{7/2}$ of Yb^{3+} ion are practically in resonance, and the probability of energy transfer between the resonant levels can be estimated as 10^7 sec^{-1} [14]).

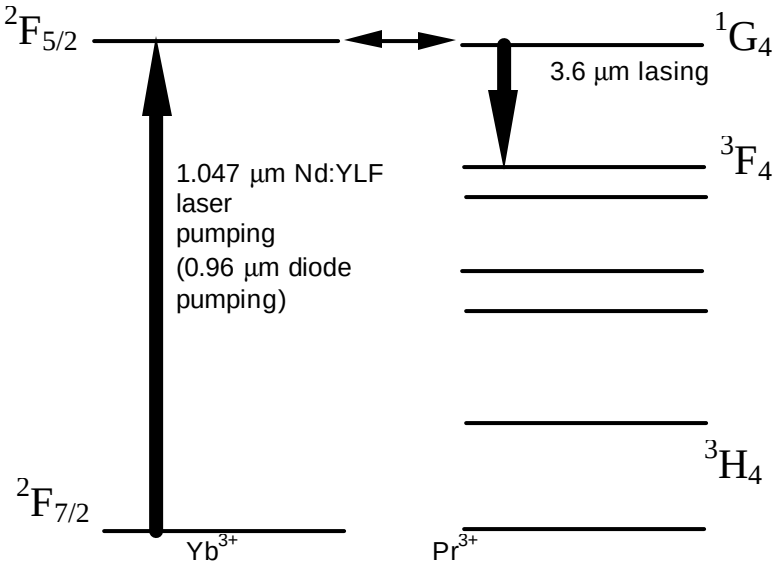

Fig. 3.1. Working scheme of active medium Yb-Pr:YLF(BYF).

Ytterbium ion has wide and intense absorption band at 0.95 μm, providing thus the opportunity to use lamp pumping. Pumping can be provided by laser diodes, emitting at 0.96 μm (absorption coefficient >5 cm^{-1}). Appropriate pump source for longitudinally pumped laser is Nd:YLF laser, emitting at 1.047 μm. Its radiation fills into the edge of the ytterbium ion band (absorption coefficient 0.3 cm^{-1} and 0.21 cm^{-1} for π and σ polarizations correspondingly in the crystal $LiYbF_4$).

In the Fig.3.1 is shown the working scheme of the active medium Yb-Pr:YLF(BYF). Energy, absorbed by sensitizer ions by means of reversible process of energy transfer is distributed between the upper laser level of praseodium ion $^1G_4$ and ytterbium ion level $^2F_{5/2}$. Excitation energy of the lower laser level of praseodium ion $^3F_4$ is subjected to the fast radiatio-less relaxation.

The relationship of probabilities of processes of direct and reversed transfer of energy between the levels $^2F_{5/2}$ of ytterbium ion and $^1G_4$ of praseodium ion can be written as:

$$\omega_{Yb\to Pr}/\omega_{Pr\to Yb} = (Z(^2F_{7/2})Z(^1G_4)/Z(^2F_{5/2})Z(^3H_4))\exp(-(E_0(^1G_4)-E_0(^2F_{5/2}))/kT),$$

or: $\omega_{Yb\to Pr}/\omega_{Pr\to Yb} = \Theta(T)$,

Here Z are the statistic sums across the sublevels of states $^2F_{7/2}$, $^1G_4$, $^2F_{5/2}$ and $^3H_4$, $E_0(^1G_4)$ and $E_0(^2F_{5/2})$ are the zero lines for the states $^1G_4$ and $^2F_{5/2}$ correspondingly. The parameter Θ, calculated on the basis of Stark structure of levels, is for the room temperature equal 18.8 and 14.8 for the crystals $LiYbF_4$:Pr and $BaYb_2F_8$:Pr correspondingly.

The probability of energy transfer is much higher than that of relaxation of excited levels, following relationship is valid for the populations of levels of each ion after excitation:

$$N(^1G_4) / N(^2F_{5/2}) = (C_{Pr}-N(^1G_4) / C_{Yb}-N(^2F_{5/2}))\,\Theta(T),$$

Here C_{Pr} and C_{Yb} are concentrations of praseodium and ytterbium ions correspondingly.

The lifetime of praseodium level $^1G_4$ in the crystals $YLiF_4$ and BaY_2F_8 equals 14 μs and 30 μs correspondingly, while that of ytterbium ion level $^2F_{5/2}$ equals 2 ms [15,16]. The common time of relaxation of the system of interacting levels $^1G_4$ and $^2F_{5/2}$ will be determined by the set of equations:

$$\begin{cases} dN_\Sigma/dt = -N(^1G_4)W(^1G_4) - N(^2F_{5/2})W(^2F_{5/2}) = N_\Sigma W_\Sigma \\ N(^1G_4) / N(^2F_{5/2}) = (C_{Pr}-N(^1G_4) / (C_{Yb}-N(^2F_{5/2}))) \Theta(T) \\ N(^1G_4) - N(^2F_{5/2}) = N_\Sigma \end{cases} \qquad \textbf{1.}$$

In the Fig.3.2 is shown the dependence of distribution of excitation between the levels $^1G_4$? $^2F_{5/2}$ – $N(^1G_4)$ / $N(^2F_{5/2})$ and of the time of excitation storage in the system of interacting levels in the crystals BaY_2F_8:Yb(10%)-Pr(0.3%) and $YLiF_4$:Yb(10%)-Pr(0.3%) upon temperature.

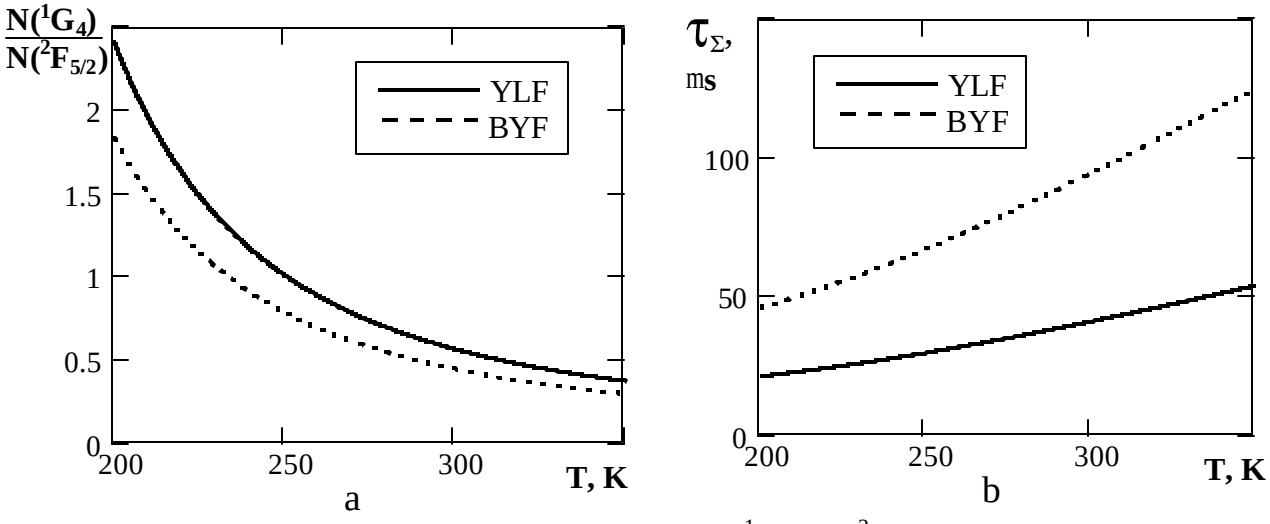

Fig.3.2. Dependence of distribution of excitation $N(^1G_4)$ / $N(^2F_{5/2})$ between the levels $^1G_4$ and $^2F_{5/2}$ (a) and of the time of excitation storage (τ_Σ) at the laser level (b) upon temperature for the crystals BaY_2F_8:Yb(10%)-Pr(0.3%) and YLF_4:Yb(10%)-Pr(0.3%).

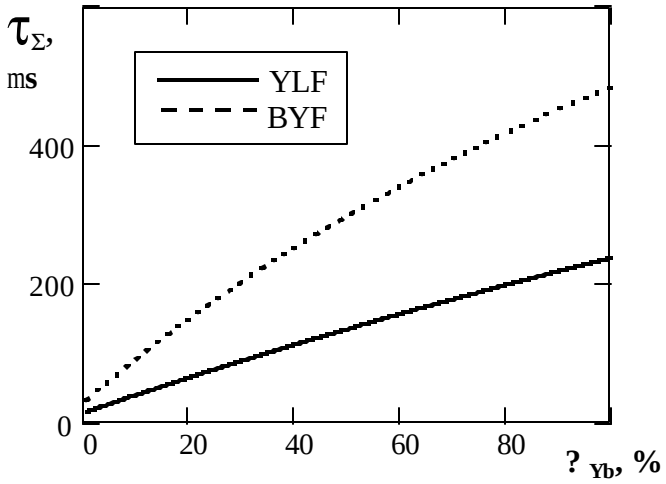

Fig. 3.3. Dependence of the time of excitation storage (τ_Σ) at the laser level upon concentration of ytterbium in the crystals BaY_2F_8:Yb-Pr(0.3%) and YLF_4:Yb-Pr(0.3%) for the temperature 300 K.

In the Fig.3.3 is shown the dependence of excitation storage in the system of interacting levels time (τ_Σ) upon ytterbium concentration in the crystals BaY_2F_8:Yb-Pr(0.3%) and YLF_4:Yb-Pr(0.3%) for the temperature 300 K. The growth of Yb concentration in crystals leads to the growth of common lifetime of levels $^1G_4$ and $F_{5/2}$, but, according to (1), the distribution of the excitation between the levels $^1G_4$ and $F_{5/2}$ is shifted to the ytterbium side.

The kinetic of working levels of crystals BYF:Yb-Pr (YLF:Yb-Pr) can be described by the system of equations:

$$\begin{cases} dN(^2F_{7/2})/dt = N(^2F_{5/2})W(^2F_{5/2}) - k1*N(^2F_{5/2})N(^3H_4) + k2*N(^2F_{7/2})N(^1G_4) - P \\ dN(^2F_{5/2})/dt = -N(^2F_{5/2})W(^2F_{5/2}) + k1*N(^2F_{5/2})N(^3H_4) - k2*N(^2F_{7/2})N(^1G_4) + P \\ dN(^3H_4)/dt = N(^1G_4)W(^1G_4) + k1*N(^2F_{5/2})N(^3H_4) - k2*N(^2F_{7/2})N(^1G_4) \\ dN(^1G_4)/dt = -N(^1G_4)W(^1G_4) - k1*N(^2F_{5/2})N(^3H_4) + k2*N(^2F_{7/2})N(^1G_4) \end{cases} \quad \textbf{2.}$$

Here k1 and k2 are the constants of direct and reversed transfer of excitation between ytterbium and praseodium, k1 / k2 = Θ, ? is the pump rate, and W is the probability of relaxation from the corresponding levels.

In the Fig.3.4. is shown the calculated dependence of amplification gain ($k_{ampl.}L_{medium}$) upon ytterbium concentration in crystals BaY_2F_8:Yb-Pr(0.3%) and YLF_4:Yb-Pr(0.3%) for the temperature 300 K. These calculations were carried out for the following parameters: pump source – Nd:YLF-laser, pumping pulse – rectangular shaped with duration 200 μs, diameter of pumped zone – 1 mm, absorbed energy – 1 J, laser transition cross-section – $\sigma = 2x10^{-21}$ cm^2 [17].

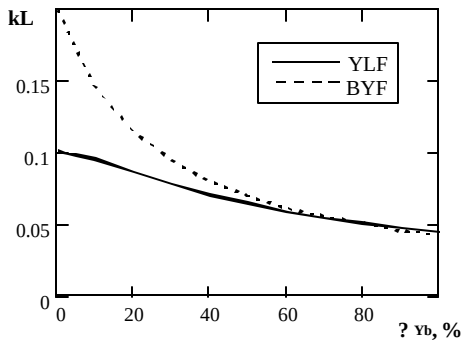

Fig.3.4. Dependence of gain increment (kL) upon ytterbium concentration in crystals BaY_2F_8:Yb-Pr(0.3%) and YLF_4:Yb-Pr(0.3%) at temperature 300 K.

Growth of ytterbium concentration leads to concentration of major part of excitation energy on ytterbium ions, leading thus to amplification reduce disrespectfully the growth of the lifetime of system of levels $^1G_4$ and $F_{5/2}$. On the other hand, the growth of Yb concentration leads to increase of medium absorption and thus the pumping efficiency increase.

In the Fig.3.5 is shown the scheme of laser setup, using the transition $^1G_4 \rightarrow {}^3F_4$ of ion Pr^{3+}. Laser crystal BaY_2F_8:Yb(10%)-Pr(0.3%) with the dimensions 3x40 mm was placed in the confocal cavity with the length 80 mm. The reflectivity of the output mirror equaled 99%. The longitudinal double-pass pumping of active element was provided by radiation from YLF_4:Nd-laser with the wavelength 1.047 μm. Pump energy was varied within the range 0.1-1.5 J. The efficiency of pumping (for absorbed energy) was equal 20%. Pumping beam diameter in active element was equal 1 mm. The generation threshold was achieved for the pump energy of 0.9 J. For the pump energy of 1.5 J the energy of generation at 3.6 μm was equal 15 mJ.

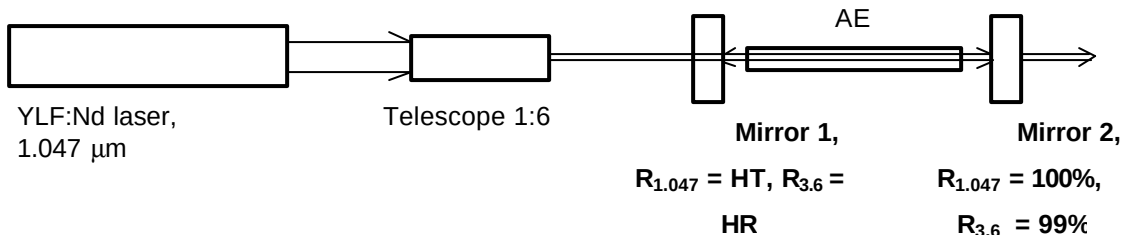

Fig.3.5. Optical scheme of laser on the base of crystal BaY_2F_8:Yb(10%)-Pr(0.3%).

So we have created the experimental model of solid-state laser on the base of crystal BaY_2F_8:Yb(10%)-Pr(0.3%) with laser pumping, providing the room-temperature generation at 3.6 μm . Generation energy 15 mJ was demonstrated for the efficiency of absorbed energy conversion into generation energy of 5%.

4. Fabrication and testing of OA LC SLMs for mid-IR radiation, addressed by visible light.

On the reported stage were also carried out the activities on testing of the first fabricated specimens of LC modulators. In the experiments was measured the value of diffraction efficiency of grating, recorded in SLM with internal mirror by visible radiation and read-out at the wavelength 2.94 μm, as well as phase retardation in SLM. The scheme of setup is shown in the Fig.4.1.

The image of test-pattern 6 was imaged to the modulator 4 in radiation of tungsten lamp 7 by the lens 6. On the first stage of the experiment the glass test pattern with the spatial frequency of 10 lines per mm (dark and transparent stripes of equal width) was used; the spatial frequency of the grating on SLM was 6 lines per mm. On the final stage of experiment it was replaced by a special test pattern with the saw-like distribution of optical density across the fringe (see Fig.4.2).

Optimal feeding voltage for the developed elements equals 4-4.5 V. The element can be fed by CW voltage, but in this case the recorded pattern is washed out. The studies have shown that in our case the optimal results were provided by feeding the modulator by the Π-shaped pulses of said voltage with the duration 0.4 sec and repetition period 0.41 sec (i.e, quasi-CW mode of operation). Reading-out Er-YAG laser was working with pulse duration 0.5 ms, highest repetition rate about 1 Hz, the energy of pulses varied in the range from 30 to 70 Hz. Parameters of BaY_2F_8:Yb-Pr laser were described in Section 3. Pulsed generation of lasers was synchronized with voltage pulses; the best results were obtained when the laser pulse came at the very end of recording pulse (0.36 sec from its beginning).

The grating was read-out as follows. The radiation from laser 1 (Er:YAG or BaY_2F_8:Yb-Pr) was reflected from the plain plates 12. These plates were mounted under the Brewster angle with respect to the radiation propagation direction and were thus selecting from the incompletely polarized laser output the component with vertical polarization. The radiation was partly reflected by the fused silica plate (not numbered) to the sensor of reference wave 11. Other part of radiation entered the modulator 4 and diffracted on the recorded grating. The diffracted wave was focused by the spherical copper mirror 8 (f=1090 mm). The energy in two diffraction orders (zeroth and first) was registered by pyro-sensors 9 and 10. The radiation of the adjustment He-Ne laser 2 entered the scheme with the assistance of removable prism on three-point basement 3.

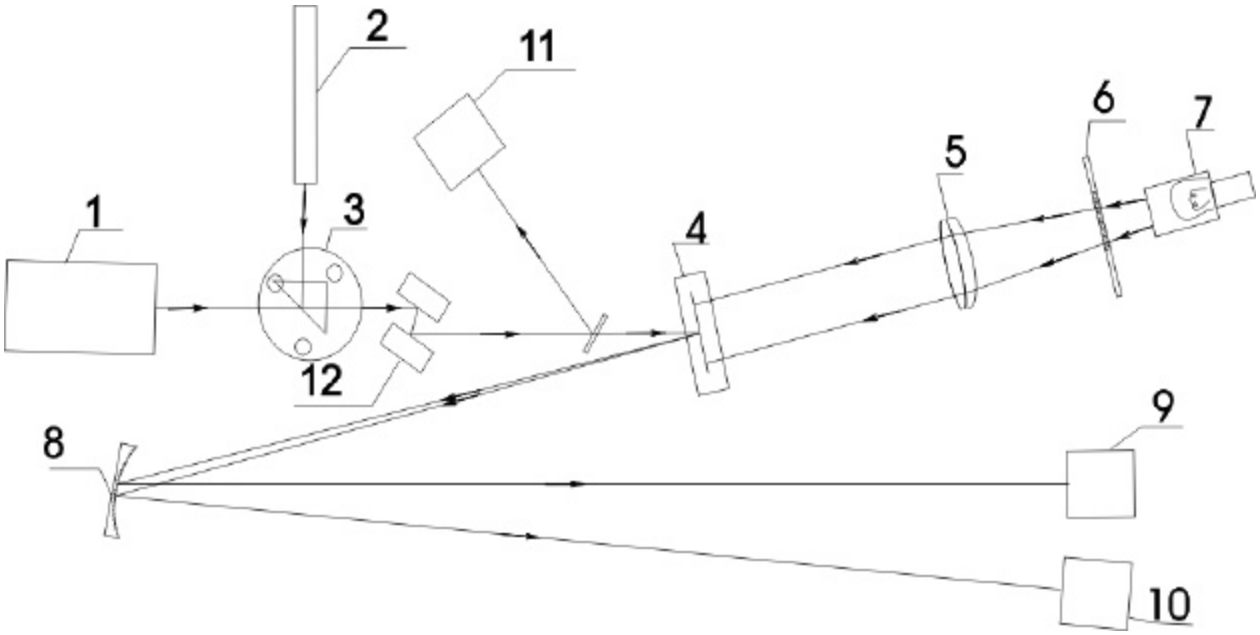

Fig.4.1. Scheme of setup for measuring the value of diffraction efficiency

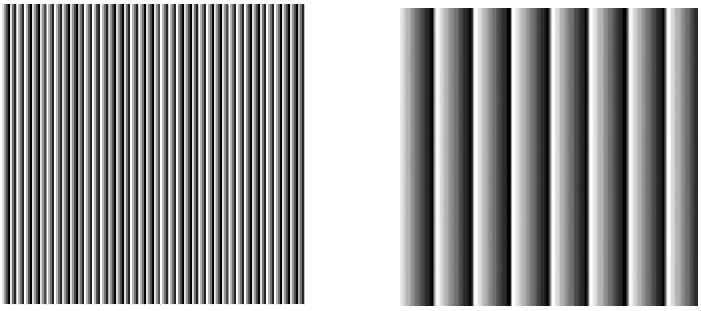

Fig.4.2. Test-object, used for recording “blazed” holographic gratings in OA SLM. The saw-like pattern was synthesized by computer (8 values of optical density, linearly distributed from complete transparency to absolutely dark) and printed at transparent film by special printer with spatial resolution 3000 lines per inch. Left – total pattern (in real scale – 2 fringes per millimeter and 3 fringes per millimeter when imaged to OA SLM), right – part of the pattern in increased scale.

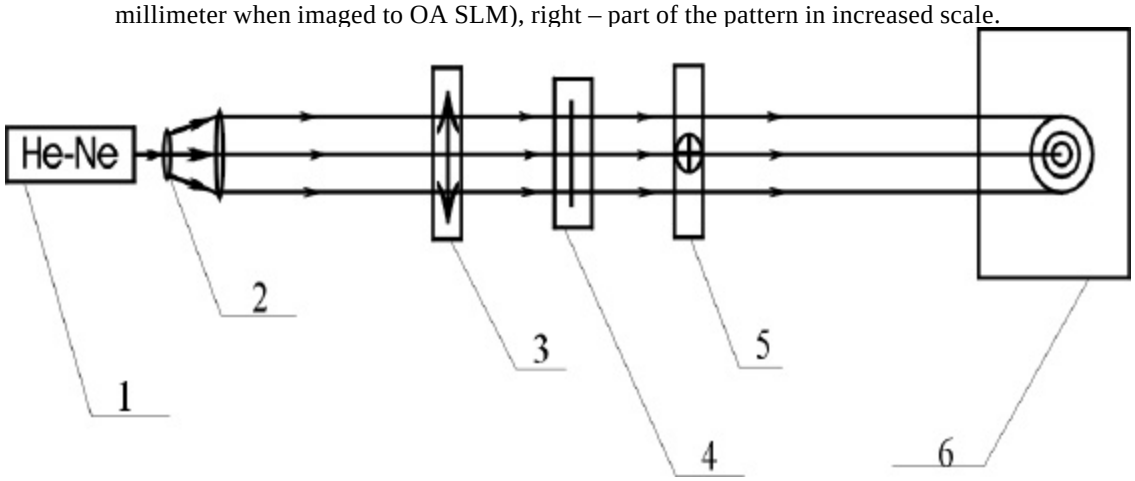

Fig.4.3. Scheme of setup for measuring the absolute value of phase retardation in OA LC SLM. In the Figure: 1 – He-Ne – laser, 2 – expanding telescope, 3 and 5 – crossed polarizers, 4 – OA LC SLM, 6 – screen.

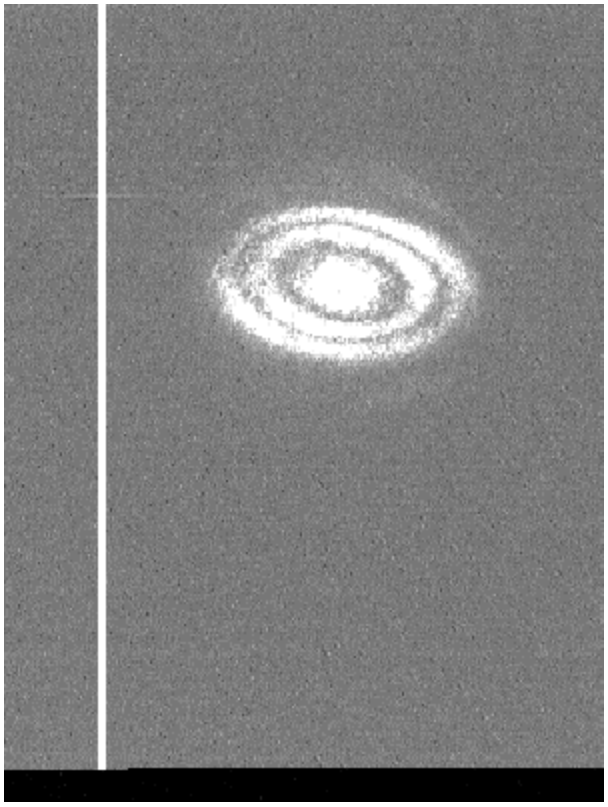

Fig. 4.4. Results of measuring of the absolute value of phase retardation

For the best of studied SLMs the measured value of diffraction efficiency equaled 12% with the use of Π-like test-pattern and was up to 70% for the saw-like test-pattern.

In addition to measurements of diffraction efficiency was also measured the value of maximal phase retardation in OA LC SLMs in visible light. With this purpose the modulators were positioned between two crossed polarizers (see Fig.4.3) and illuminated by the expanded beam of He-Ne laser at 632 nm with the Gauss-like intensity distribution. The value of maximal phase retardation was evaluated from the number of rings on the screen. These measurements were made in transparency mode, because the reflectivity of internal mirror for visible light was low. In the Fig.4.4 is shown one of registered ring-shaped structures. One can see that for visible light the maximal value of phase retardation is ~6p; consequently, for the reflective mode of modulator operation the value of phase retardation is ~12p for the wavelength 632 nm and over 2p for mid-IR range of 3-4 μm.

Conclusion

In conclusion we can say that in course of work were developed and tested the specimens of liquid crystal phase spatial light modulators for the spectral range 3-4 μm, optically addressed by visible radiation, meeting the technical requirements of the Contract. The best of fabricated elements provided over 2π phase retardation in the said spectral range and high diffraction efficiency of gratings with symmetrical (up to 12%) and asymmetrical (up to 70%) fringe profile.

The results of the reported work can become the basis for the development of OA SLMs of new kinds. At this moment we see three important problems and ambitious goals, which can and are to be solved on the possible next stages of investigations:

1. Numerous possible applications of OA LC SLMs and dynamic holograms in such elements are related to the use of laser radiation. However, all developed elements are characterized by the comparatively low optical damage threshold, and first of all due to the vulnerability of the transparent electrode layer.
2. The elements, designed within the scope of the reported work, were based on the use of the comparatively slow chalkogenide glass photoconductor layer. The results of other efforts, in particular, the results of the ISTC Project 2101p, indicate that there is an opportunity to realize, at least in near-IR spectral range, the 2π-phase retardation with the use of much quicker silicon carbide photoconductor.
3. New ambitious opportunities to work in the very interesting spectral range 3-3.5 μm and in other spectral regions, where the traditional hydrogen containing media reveal intense absorption (for instance, nearby 1.06 μm), may open with synthesis and application of deuterium-replaced liquid crystals (see Section 1).

To our opinion, the most important task for today is to create on the base of existing and recently developed technologies the elements, applicable for use with radiation of Nd-lasers (1.04-1.08 μm) and various eye-safe lasers, emitting nearby 1.55 μm. These can be the elements, recorded by visible light in the schemes, discussed in Section 1, providing 2π retardations in the said spectral regions and implementing some novel elaborations, aimed onto increase of admissible controlled energy. To our opinion the 1-year effort with approximate cost of US

$60.000-80.000 can results in creation of elements with clear aperture~25-30 mm for control of radiation in spectral regions 1-1.1 μm and/or about 1.5 μm. Such an effort should comprise:

1. Analysis of limitations of optical damage threshold of transparent electrodes and of other layers of OA LC SLM. Theoretical and experimental study of the possibility to replace the standard transparent electrode material (ITO) by other conducting oxides.
2. Analysis of other limitations of admissible energy of controlled radiation, in particular, of the residual sensitivity of various photoconducting layers at the wavelength of reading out IR radiation.
3. Fabrication and testing of several specimens of OA LC SLMs, providing 2π-retardation and high diffraction efficiency of dynamic gratings in the spectral range 1-1.1 μm and/or around1.55 μm.

On completion of such a one-year effort it can be then continued by modification of existing technologies with regard to results of investigations within the scope of items 1 and 2 and extension of clear aperture of OA LC SLMs up to 50-80 mm.

References

1. Berenberg V.A., Leshchev A.A., Soms L.N., Vasil'ev M.V., Venediktov V.Yu., Onokhov A.P., Beresnev L.A. Polychromatic dynamic holographic one-way image correction using liquid crystal SLMs// Optics Communications.-1999.-Vol. 166.-P. 181-188.
2. Gruneisen M.T., Peters K.W., Wilkes J.M. Compensated imaging by real-time holography with optically addressed liquid-crystal spatial light modulators// Proc. of SPIE.-1997.-Vol. 3143.-P. 171-181.
3. Berenberg V.A., Leshchev A.A., Semenov P.M., Vasil'ev M.V., and Venediktov V.Yu. Correction of Telescope's Primary using Dynamic Holography in Optically Addressed Liquid Crystal Spatial Light Modulator// Molecular Crystals and Liquid Crystals.-2000.-Vol. 351-P. 9-16.
4. Vasil'ev A.A., Kassasent D., Kompanetz I.N., and Parfenov A.V. *Spatial light modulators* (Radio i svyaz, Moscow, 1987, in Russian).
5. Wick D.V., Martines T., Wood M.V., Wilkes J.M., Gruneisen M.T., Berenberg V.A., Vasil'ev M.V., Onokhov A.P., Beresnev L.A. Deformed-helix ferroelectric liquid-crystal spatial light modulator that demonstrates high diffraction efficiency and 370-line pairs/mm resolution// Applied Optics.-1999.-Vol. 38, No. 17.-P. 3798-3803.
6. Berenberg V.A., Beresnev L.A., Chaika A.N., Feoktistov N.A., Gruneisen M.T., Isaev M.V., Konshina E.A., Onokhov A.P. OA LC SLM with high net optical efficiency for holographic correction of distortions// Proc. of SPIE.-2000.-Vol. 4124-P. 265-268.
7. Venediktov V.Yu., Berenberg V.A., Danilov V.V. et al. Holographic correction in mid-IR using OA LC SLM elements Proc.of SPIE, **4124** (2000) 257.
8. Toyoda H., Kobayashi Y., Yoshida N., Igasaki Y., Hara T., Ishikawa M, Wu M.H. High efficient electrically-addressable spatial light modulator for reconfigurable optical interconnection// OSA Snowmass Meeting, SLM'99 technical digest, SMB3.
9. Percheron I., Baker J.T., Gruneisen M., Martinez Ty, Wick D. Blazed holographic optical aberration compensation// Proceedings of the 2nd International Workshop on Adaptive Optics for Industry and Medicine, ed. By Gordon D.Love, World Scientific, Singapore – New Jersey – London – Hong Kong-1999.-P. 384-387.
10. Frisch M.J., Trucks G.W., Schlegel H.B., Scuseria G.E., Robb M.A., Cheeseman J.R., Zakrzewski V.G., Montgomery J.A., Stratmann Jr., R.E., Burant J.C., Dapprich S., Millam J.M., Daniels A.D., Kudin K.N., Strain M.C., Farkas O., Tomasi J., Barone V., Cossi M., Cammi R., Mennucci B., Pomelli C., Adamo C., Clifford S., Ochterski J., Petersson G.A., Ayala P.Y., Cui Q., Morokuma K., Malick D.K., Rabuck A. D., Raghavachari K., Foresman J. B., Cioslowski J., Ortiz J.V., Baboul A. G., Stefanov B. B., Liu G., Liashenko A., Piskorz P., Komaromi I., Gomperts R., Martin R.L., Fox D.J., Keith T., Al-Laham M. A., Peng C. Y., Nanayakkara A., Gonzalez C., Challacombe M., Gill P. M. W., Johnson B., Chen W., Wong M. W., Andres J. L., Gonzalez C., Head-Gordon M., Replogle E.S., Pople J.A. *Gaussian 98, Revision A.7*. Gaussian, Inc.: Pittsburgh PA. 1998.
11. Becke A.D. Density functional exchange energy approximation with correct asymptotic behavior. //Physical review. A. 1988. V. 38. P. 3098-3100.
12. Perdew J.P., Wang Y. Accurate and simple analytic representation of the electron gas correlation energy. //Physical review. B. 1992. V. 45. P. 13244.

13. A.A.Kaminsky, K.Kurbanov, T.V.Uvarova, Izvestiya AN SSSR, Nonorganic substances. 1987. V.23. P.1049 (in Russian).
14. B.M.Antipenko, A.A.Mak, V.B.Nikolaev, O.B.Raba, K.B.Seyranyan, T.V.Uvarova. Optika i spektroskopiya, 1984. V.56. P.484 – 489(in Russian).
15. T.T. Basiev, Yu.V. Orlovskii, K.K. Pukhov, V.B. Sigachev, M.E. Doro shenko, and I.N. Vorob'ev, "Multiphonon relaxation in the rare-earth ions doped laser crystals," OSA Trends in Optics and Photonics Series, Advanced Solid-State Lasers, Washington, D.C., **1,** pp. 575-581, 1996
16. R.H. Page, K.I. Schaffers, G.D. Wilke, J.B. Tassano, S.A. Payne, and W.F. Krupke, "Spectroscopy and Decay Kinetics of Pr^{3+}-Doped Chloride Crystals for 1300 nm Optical Amplifiers," Advanced Solid-State Lasers, OSA Proceedings, Washington, D.C., **24**, pp.514-518, 1995.
17. A.A.Mak, B.M.Antipenko. Rare-earth converters of neodymium laser radiation spectrum. Journal of Applied Spectroscopy. 1982. V.37. No.6. P.1029-1045(in Russian).

Publication of Project Results

The results of the Project became the basis for two reports at International Conferences (the XIV International Symposium On Gas Flow & Chemical Lasers and High Power Laser Conference, Wroclaw, Poland, 25-30, August 2002 and the 9th International Symposium on Remote Sensing, 22-27 September 2002, Agia Pelagia, Crete, Greece). The presentation at the second meeting became also the basis for the paper, submitted to the Proceedings of SPIE, vol.4884. The abstracts for the said two presentations and for the said paper are given further.

1. **The talk at the XIV International Symposium On Gas Flow & Chemical Lasers and High Power Laser Conference, Wroclaw, Poland, 25-30, August 2002 (only oral presentation)**

Title: Dynamic holographic correction in laser systems: new schemes and technologies

Authors: V.Yu.Venediktov, V.A.Berenberg

Abstract: The paper considers several new concepts of dynamic holographic correction schemes and new technologies of liquid crystal valves for such correction, which can be useful in high average power laser systems.

Summary:

Standard schemes and methods of dynamic holographic correction of distortions in high average power lasers, based on the use of efficient thin dynamic holograms in optically addressed liquid crystal spatial light modulators (OA LC SLMs, see, for instance, [1]), are subjected to some limitations. These are, first of all, limited diffraction efficiency (not more than 30-35% for standard schemes of holographic record) and spectral region of performance, limited, in fact, by the visible spectral range.

We consider several novel approaches, providing solution of both problems. These are first of all several novel schemes, providing the record of dynamic holograms with asymmetrical fringe profile (“blazed” dynamic holograms) and thus

providing much higher value of diffraction efficiency (in theory – up to 100%). One can also extend the spectral range of method applicability by use of novel schemes with TV (computer) relay of interferogram or by means of the so-called double-wavelength dynamic holography.

We also discuss some novel advances in architecture and technology of OA LC SLMs, first of all of the elements, specially developed for the purposes of "blazed" dynamic holography and for correction in near- and mid-IR ranges of spectrum. In such elements, unlike traditional valves, the internal mirror is positioned not between LC and photoconductor layers, but beyond photoconductor. Significant difference of wavelength of dynamic hologram record and reading-out, which is possible in the said schemes with TV (computer) relay of interferogram and on the base of the double-wavelength dynamic holography, permits the use of mirrors, transparent for visible light. First specimens of such elements have provided the diffraction efficiency in ~10% for radiation at 2.94 μm.

1. V.A.Berenberg, A.A.Leshchev, L.N.Soms, M.V.Vasil'ev, V.Yu.Venediktov, Adaptive system of laser energy transport with OA LC SLM correction element, Proc. SPIE, 4184, 465-468 (2000).

2. **The talk at the 9th International Symposium on Remote Sensing, 22-27 September 2002, Agia Pelagia, Crete, Greece and the paper in Proceedings of SPIE, vol.4884, paper 50.**

Title: New elements and schemes for holographic correction in mid-IR

Authors: Vladimir Berenberg, Vladimir Venediktov, Nikolay Freygang, Yury Petrushin, Larisa Amosova, Nina Pletneva, Mark Gruneisen

Abstracts: We discuss several schemes and methods, providing the possibility to extend the method of dynamic holographic correction of distortions by means of optically addressed liquid crystal spatial light modulators (OA LC SLMs) to IR spectral range. These are first of all the schemes with TV (computer) relay of interferogram to modulator and double-wavelength dynamic holography schemes. We consider also the performance of first OA LC SLMs, specially developed for correction in 2.5-4 μm spectral range, providing diffraction efficiency of ~10% in traditional scheme and about 75% in the case of grating with asymmetric profile.

Information on patent and copyrights

In accordance with the Contract and Work Plan provisions no patent applications were filed or other protection documents were signed.